

# Analysis of Hepatitis B Viral Load Decline Under Potent Therapy: Complex Decay Profiles Observed

SHARON R. LEWIN,<sup>1,2</sup> RUY M. RIBEIRO,<sup>3</sup> TOMOS WALTERS,<sup>4</sup> GEORGE K. LAU,<sup>5</sup>  
SCOTT BOWDEN,<sup>4</sup> STEPHEN LOCARNINI,<sup>4</sup> AND ALAN S. PERELSON<sup>3</sup>

We used a new real-time polymerase chain reaction (PCR)-based assay that is sensitive, has a wide dynamic linear range, and is highly reproducible to quantify hepatitis B virus (HBV) DNA in the serum of infected individuals undergoing potent antiviral therapy. In addition, we made frequent measurements of viral load after initiation of treatment and maintained follow-up to about 12 weeks. To analyze the data we used a new model of HBV decay, which takes into account that existing drug treatments do not completely block *de novo* infection and the possibility of noncytolytic loss of infected cells. On initiation of therapy, there was a mean delay of 1.6 days followed by a biphasic or multiphasic decay of plasma HBV DNA. The slope of the first phase varied considerably, with one individual having rapid decay, corresponding to a virion half-life of 1 hour, but others showing half-lives of up to 92 hours. Individuals either had a slow second-phase decline ( $t_{1/2} = 7.2 \pm 1.2$  days) or a flat second phase. Some individuals exhibited a complex “staircase pattern” of decay, with further phases of viral DNA decline and phases with little change in viral load. (HEPATOLOGY 2001;34:1012-1020.)

Analysis of viral dynamics during antiviral therapy has been critical to the understanding of the pathogenesis of several blood-borne viruses including human immunodeficiency virus (HIV), hepatitis C virus (HCV), and hepatitis B virus (HBV).<sup>1-7</sup> Pathogenesis of each of these viruses is characterized by a dynamic equilibrium between virus production and clearance. By disturbing this equilibrium with antiviral therapy and by mathematically analyzing the resulting decline in plasma viral load, insight has been gained into viral dynamics

*in vivo*. In the case of HIV, the virion clearance rate and the rate of loss of infected cells derived from these analyses have been minimal estimates because they were based on the assumption that drug penetration is complete and that antiviral therapy is 100% effective. In the case of HCV and HBV it has not been necessary to assume that therapy is 100% effective, yet it has been possible to estimate the virion clearance rate, the infected cell loss rate, and the effectiveness of the therapy in blocking virion production. In the case of HIV and HCV, parameter estimates obtained by using viral dynamic theory have been independently confirmed by methods such as quantitative image analysis of tissue samples<sup>8,9</sup> and plasma apheresis.<sup>10</sup> However, the application of viral dynamic theory to HBV viral load measurements made in individuals on antiviral therapy is still in its early stages, and the conclusions drawn from these kinetic analyses still await experimental confirmation.

A number of nucleoside analogues such as lamivudine (LMV),<sup>11</sup> famciclovir (FCV),<sup>12,13</sup> and adefovir dipivoxil<sup>7,14</sup> have been shown to be effective in suppressing HBV replication *in vivo*. A recent study of antiviral therapy for HBV showed enhanced efficacy of combination therapy with LMV and FCV as compared with LMV alone.<sup>15</sup> We performed a viral dynamic analysis on these same individuals, but used a molecular beacon assay<sup>16,17</sup> that accurately quantifies viral load over a wide dynamic range to further characterize the half-life of free virions and infected cells for each individual. Our analysis shows a heterogeneous and complex pattern of HBV viral decay.

After treatment of HBV with antiviral agents, a biphasic decline in viral load has been reported, with an initial rapid decline representing decay of HBV virions followed by a slower second phase representing the clearance of infected cells.<sup>5-7</sup> The current estimates of the half-life of HBV virions have a mean value of 24 hours,<sup>5,6,15</sup> whereas the reported mean half-life of infected cells ranges from 10 to 100 days.<sup>5,7</sup> The estimates of the half-life of HBV virions are significantly longer than those of either HIV ( $t_{1/2} < 6$  hours by drug perturbation experiments and  $\sim 1$  hour by plasma apheresis<sup>10</sup>) or HCV ( $t_{1/2} \sim 2-3$  hours by both drug perturbation<sup>4</sup> and apheresis experiments<sup>10</sup>). This is surprising given that the size of HBV particles (diameter, 42 nm) and HCV particles (diameters of 45 to 65 nm have been observed in humans and chimpanzees<sup>18,19</sup>) are similar, and there appears to be a correlation between viral particle size and efficiency of clearance (see Nathanson and Tyler<sup>20</sup> and references therein). In this report we show that in one HBV-infected individual drug perturbation does indicate fast clearance ( $t_{1/2} \sim 1$  hour), whereas in

---

Abbreviations: HIV, human immunodeficiency virus; HCV, hepatitis C virus; HBV, hepatitis B virus; LMV, lamivudine; FCV, famciclovir; HBeAg, hepatitis B e antigen; PCR, polymerase chain reaction; cccDNA, covalently closed circular DNA; ALT, alanine transaminase.

From the <sup>1</sup>Victorian Infectious Diseases Service and <sup>4</sup>Victorian Infectious Diseases Reference Laboratory, The Royal Melbourne Hospital, Parkville, Victoria, Australia; <sup>2</sup>Department of Microbiology and Immunology, The University of Melbourne, Parkville, Victoria, Australia; <sup>3</sup>Los Alamos National Laboratory, Los Alamos, NM; <sup>5</sup>Department of Medicine, Queen Mary Hospital, Hong Kong, People's Republic of China.

Received May 18, 2001; accepted August 6, 2001.

Portions of this work were done under the auspices of the U.S. Department of Energy. Supported by NIH grant RR06555. S.R.L. is supported by the National Health and Medical Research Council of Australia, and The Ian Potter Foundation.

S.R.L. and R.M.R. contributed equally to this work.

Address reprint requests to: Alan S. Perelson, Ph.D., Theoretical Division, MS-K710, Los Alamos National Laboratory, Los Alamos, NM 87545. E-mail: asp@lanl.gov; fax: 505-665-3493.

Copyright © 2001 by the American Association for the Study of Liver Diseases.

0270-9139/01/3405-0020\$35.00/0

doi:10.1053/jhep.2001.28509

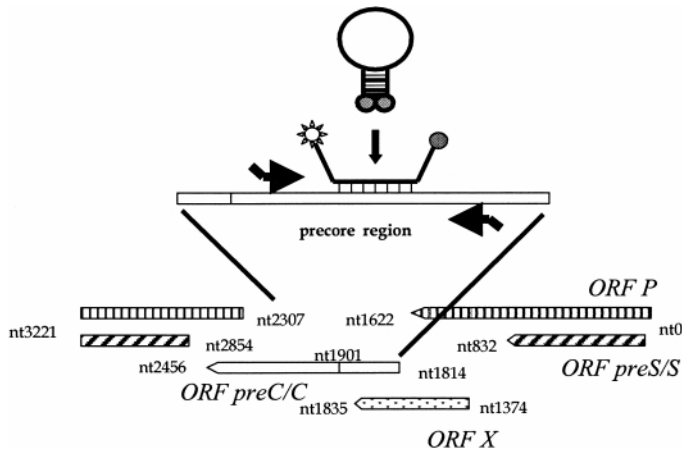


FIG. 1. Location of primers and the molecular beacon on the HBV genome, with nucleotides numbered from the cleavage site of EcoRI. PC1 hybridizes to nucleotides 1744-1761, PC2 to nucleotides 1940-1959, and the molecular beacon to nucleotides 1854-1879. The Victorian Infectious Diseases Reference Laboratory (VIDRL) HBV sequence database (Dr A. Bartholomeusz, VIDRL, Melbourne, Australia, personal communication) shows these regions to be well conserved across all HBV genotypes.

other individuals, clearance is much slower. Thus, some process may be slowing HBV clearance. Further, we show that the pattern of HBV DNA decay can be more complex than the typical biphasic pattern, with some patients exhibiting additional phases, raising questions about the need to improve the basic viral dynamic model. We suggest that including both cytolytic and noncytolytic mechanisms of infected cell loss will make models more realistic as well as more accurate.

#### PATIENTS AND METHODS

**Patient Details.** Fifteen subjects chronically infected with HBV from Nanfang Hospital, Guangzhou, and the Queen Mary Hospital, Hong Kong, were studied. Informed consent was obtained from the patients. Subjects were treated with either LMV monotherapy (LMV 150 mg/d) or LMV/FCV combination therapy (LMV 150 mg/d, FCV 500 mg 3 times a day). All patients were hepatitis B e antigen (HBeAg)-positive on 2 occasions before the start of therapy. Individuals received therapy for 12 weeks and serial serum samples were taken at days 0, 1, 2, 3, 4, 5, 6, 7 or 8, and 9 or 10, and at weeks 2, 4, 6, 8, 10, and 12. Further sera were drawn from certain patients after the completion of therapy. Of the 15 individuals included in this study of viral dynamics, 10 were treated with LMV/FCV combination therapy and 5 with LMV monotherapy. The clinical and virologic outcome of this study—using the Digene Hybrid-Capture II Assay (Digene Diagnostics, Beltsville, MD) to measure HBV DNA—was published elsewhere.<sup>15</sup>

**Quantification of HBV DNA in Plasma.** For the real-time polymerase chain reaction (PCR)-based assay for HBV, HBV DNA was extracted from 200  $\mu$ L of serum using the QIAamp DNA Mini Kit according to the manufacturer's instructions (QIAGEN GmbH, Hildens, Germany). Primers and a molecular beacon were designed for conserved nucleic acid sequences within the precore domain of the HBV genome to amplify and detect a 216-nucleotide product (Fig. 1). Amplification was performed in a 50- $\mu$ L reaction mixture containing 1.0  $\times$  Taqman buffer A (Applied Biosystems, Foster City, CA), 3.0 mmol/L MgCl<sub>2</sub>, 0.4 pmol of each primer per  $\mu$ L, forward primer: PC1 (5'-GGGAGGAGATTAGGTAA-3') and reverse primer: PC2 (5'-GGCAAAAACGAGAGTAACTC-3'), 0.4 pmol of the HBV-specific molecular beacon per  $\mu$ L, (5'-FAM-CGCGTCCTACTGTTCAAGCCTCCAAGCTGTGACGCG-DABCYL-3', where FAM represents fluorophore 6-carboxyfluorescein and DABCYL, 4-dimethylaminophenylazobenzoic acid, a quenching chromophore), and 1.25 U of

AmpliQaq Gold DNA polymerase (Perkin-Elmer, Norwalk, CT). PCR was performed using the ABI PRISM 7700 spectrofluorometric thermocycler (Applied Biosystems). The PCR program consisted of an initial cycle (95°C for 10 minutes) followed by 45 amplification cycles (94°C for 15 seconds, 50°C for 30 seconds, and 72°C for 30 seconds). The instrument detected and recorded the fluorescence spectrum of each reaction tube during the annealing phase.

An external standard was constructed by ligation of a 1.3-kb wild-type HBV plasmid (genotype D) into the pBlueBac plasmid vector (kind gift from Dr. Delaney, Hershey Medical Center, Hershey, PA). Quantification of the DNA concentration of the plasmid was determined by spectrophotometry. Duplicates of serial 10-fold dilutions of the plasmid ranging from 10<sup>8</sup> copies/mL to 100 copies/mL were included in each run to generate a standard curve. The copy number in each experimental reaction was determined by interpolation of the derived threshold cycle ( $C_T$ ), as previously described.<sup>17,21-23</sup>

HBV Digene Hybrid Capture II microplate assay and the Cobas AMPLICOR HBV MONITOR assay (Roche, Branchburg, NJ) were performed in accordance with the instructions of the manufacturer. For the HBV Digene Hybrid Capture microplate assay, the lower detection limit of the assay was 0.5 pg (equivalent to 1.42  $\times$  10<sup>5</sup> copies/mL). The ultrasensitive format of the assay was not used because of restriction on the amount of serum volume available. For the HBV MONITOR assay the detection limit of the assay, according to the manufacturer, was 200 genome equivalents per mL. The dynamic range of the assay was 2  $\times$  10<sup>2</sup> to 4  $\times$  10<sup>5</sup> genome equivalents per mL. For higher concentrations, dilutions of the input DNA were performed as recommended by the manufacturer.

**Drug-Resistant Quasispecies.** Amino acid changes in the polymerase at M550V/M550I, associated with LMV resistance, and L526M, associated with FCV resistance, were assessed before treatment and after 12 weeks of treatment. The Inno LiPA HBV DR Amplification assay (Innogenetics N.V., Ghent, Belgium) was used according to the manufacturer's instructions. Briefly, the assay is a PCR-based, reverse hybridization line probe assay that allows qualitative detection of genomic mutations corresponding to amino acid changes at positions 550 and 526 in the HBV polymerase enzyme.<sup>24</sup>

**Mathematical Model.** The experimental data were analyzed with a generalization of a model used before by us and others.<sup>4,5,7</sup> In the model, illustrated in Fig. 2, the dynamics of uninfected target cells ( $T$ , presumably hepatocytes), infected cells ( $I$ ) and free virions ( $V$ ) are considered. The equations for these populations are:

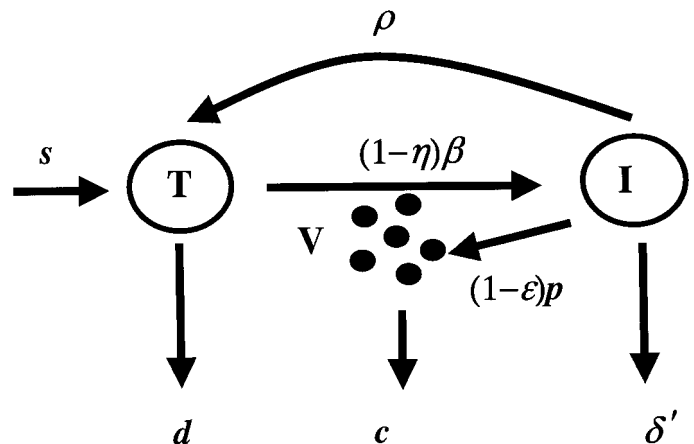


FIG. 2. Diagrammatic representation of the mathematical model for HBV treatment. Model depicts target cells,  $T$ ; infected cells,  $I$ ; and HBV virions,  $V$ . Model parameters are  $d$  = death rate of target cells,  $\delta'$  = death rate of infected cells;  $\rho$  = rate of "cure," i.e., noncytolytic loss of infected cells; ( $\delta' + \rho = \delta$  = net loss rate of infected cells);  $c$  = clearance rate of free virions;  $\epsilon$  = efficiency of drug therapy in inhibiting viral production;  $\eta$  = efficiency of drug therapy in preventing new infections;  $p$  = rate of production of virions per infected cell;  $\beta$  = rate of infection of new target cells;  $s$  = rate of production of new target cells.

$$\begin{aligned} \frac{dT}{dt} &= s - dT - (1 - \eta)\beta VT + \rho I \\ \frac{dI}{dt} &= (1 - \eta)\beta VT - \delta' I - \rho I \\ \frac{dV}{dt} &= (1 - \epsilon)pI - cV \end{aligned} \quad (1)$$

We assume that target cells are created at rate  $s$  and die at rate  $d$  per target cell. These cells are infected at rate  $\beta$  per uninfected cell per virion. Infected cells die at rate  $\delta'$  per cell, which may be different from the uninfected cell death rate because of viral or immune effects. In addition, infected cells may also revert to the uninfected state by loss of all covalently closed circular DNA (cccDNA) from their nucleus,<sup>25</sup> at a rate  $\rho$  per infected cell. Thus the total rate of disappearance of infected cells is  $\delta = \delta' + \rho$ . Infected cells produce virions at an average rate  $p$  per infected cell, and viral particles are cleared from the circulation at rate  $c$  per virion. In this model, as in previous ones,<sup>5-7</sup> the virion production rate is assumed to be constant. In more complex models that also keep track of the number of copies of cccDNA per cell the production rate could be made proportional to the cccDNA content of a cell. However, because of lack of data on cccDNA copy number, this has not been done here.

Treatment with LMV or FCV inhibits the reverse transcription step needed for the formation of new virions. This means that under drug therapy the production rate of new virions,  $p$ , is decreased. We define the drug efficacy,  $\epsilon$ , such that the virion production rate under therapy is  $(1 - \epsilon)p$ . A drug that is 100% ( $\epsilon = 1$ ) efficient results in complete suppression of new virion production. Although the viral polymerase, which is inhibited by LMV or FCV, may possibly help in the formation of cccDNA, cellular polymerases appear to be sufficient to close the single stranded gap in the relaxed circular viral genome<sup>26</sup> and other cellular factors can then convert the structure into cccDNA.<sup>27</sup> If this is the case, then *de novo* infection of uninfected cells may be largely unimpaired in the presence of reverse transcriptase inhibitors. However, a recent report<sup>28</sup> suggests that lamivudine may have a small effect in blocking infection. To incorporate the possibility of LMV or FCV affecting infection, we introduce a parameter that accounts for the efficacy of the drug in blocking new infection,  $\eta$ , so that the infection rate in the presence of drug is  $(1 - \eta)\beta$ . To fit this model to the data, we used  $\eta = 0.5$  (see the Discussion).

To solve the model equations, we assume that during the course of therapy, which only lasts 12 weeks, the number of target cells remains approximately constant and that the individual is initially at steady state. In the solution we also account for the possibility of an initial delay existing between the start of treatment and its effect in reducing viral load, due to pharmacokinetics or the intrinsic viral life cycle time. This is accounted for in the model by allowing a temporal delay ( $\tau$ ) between the start of treatment and the initial decline of virus load.<sup>4</sup> The solution is then given by:

$$V(t) = \frac{1}{2}V_0 \left[ \left( 1 - \frac{c + \delta - 2\epsilon c}{\theta} \right)^{-\lambda_1(t-\tau)} + \left( 1 + \frac{c + \delta - 2\epsilon c}{\theta} \right) e^{-\lambda_2(t-\tau)} \right], \quad (2)$$

where  $\lambda_1$ ,  $\lambda_2$  (the eigenvalues) are given by  $1/2(c + \delta + \theta)$  and  $1/2(c + \delta - \theta)$ , respectively, and  $\theta = \sqrt{(c - \delta)^2 + 4(1 - \epsilon)(1 - \eta)c\delta}$ . This solution is valid for  $t > \tau$ . For  $t < \tau$ , the solution is  $V(t) = V_0$ , where  $V_0$  is the initial viral load. This model is fit to the data by using nonlinear least squares regression to find the parameters that best describe the data. From the fits we obtain the parameters,  $\delta$ , and  $c$ . From these we calculate the infected cell and virion half-lives ( $t_{1/2}$ ), given by  $\ln(2)/\delta$  and  $\ln(2)/c$ , respectively, where the natural logarithm of 2,  $\ln(2) \approx 0.693$ .

**Data Analysis and Statistics.** The nonparametric Wilcoxon rank sum test was used to determine statistical significance of differences between groups of patients. The Spearman nonparametric test was used to assess the correlation between continuous variables.

## RESULTS

**Real-Time PCR Assay for HBV Is Sensitive, Has a Wide Dynamic Linear Range, and Is Highly Reproducible.** The molecular beacon and real-time PCR-based assay provided accurate quantification of serum HBV DNA concentration ranging from  $10^2$  copies/mL to  $10^9$  copies/mL. The assay variation for DNA extraction and amplification was determined by the analysis of HBV-infected sera from 15 individuals with low (0.5-10 pg/mL,  $\sim 10^5$ - $10^6$  copies/mL,  $n = 5$ ), medium (10-200 pg/mL,  $\sim 10^6$ - $10^7$  copies/mL,  $n = 5$ ), and high (200-500 pg/mL,  $\sim 10^7$ - $10^8$  copies/mL,  $n = 5$ ) levels of HBV DNA, as measured by the Digene-Hybrid Capture II assay. DNA from sera of each individual was extracted on 5 occasions, and HBV DNA from each extraction was quantified in 5 separate real-time PCR runs. The coefficient of variation of the assay for HBV DNA quantification alone, over the 5 separate runs for each extraction, was  $0.21 \pm 0.05$  (mean  $\pm$  SD,  $n = 15$ ). The corresponding coefficient for the sum of interassay variation for both DNA extraction and quantification, over the 25 measurements in each patient, was  $0.35 \pm 0.08$  (mean  $\pm$  SD,  $n = 15$ ). There was no significant difference in the coefficient of variation for extraction or quantification of HBV from sera with low, medium, or high levels of HBV DNA.

The real-time PCR assay for HBV was compared with two commercially available assays. Twenty-six samples were tested in both the real-time PCR assay and the Digene Hybrid Capture II assay. There was a strong correlation between the real-time PCR assay and the Digene Hybrid Capture II assay at high ( $> 10^6$  copies/mL) viral loads ( $r = 0.93$ ,  $P < .001$ ; Fig. 3B), but there was little correlation at the lower limits of sensitivity of the Digene assay, namely at viral loads between  $10^5$  copies/mL and  $10^6$  copies/mL (data not shown). Twenty samples were compared with the Cobas HBV AMPLICOR MONITOR assay. All samples were within the range of the HBV MONITOR assay. The real-time PCR assay showed a strong correlation with the HBV MONITOR assay ( $r = 0.94$ ,  $P < .001$ ; Fig. 3A). The mean of the differences in the log-transformed data for the real-time PCR assay and the Digene Hybrid Capture II assay was  $0.08 \pm 0.22$  and with the HBV MONITOR assay was  $0.11 \pm 0.45$ . In summary, the real-time PCR-based assay using molecular beacons was sensitive, had a wide dynamic range, was reproducible, and showed a strong correlation with 2 commercially available assays in their optimal but restricted range. This real-time PCR assay with molecular beacons had similar features and performance characteristics to assays for HBV DNA using Taqman probes, which have recently been reported.<sup>29,30</sup>

**Biphasic Decay in HBV DNA After Antiviral Therapy Is Variable Among Individuals.** In most individuals, after treatment with either LMV or LMV/FCV 2 phases could be distinguished in the HBV DNA decay curve (Fig. 4A and B). The behavior in these 2 phases, however, is variable and the individual dynamic parameters show heterogeneity (Table 1). Individuals may be divided into 2 groups depending on whether they have a slow second-phase decay or no decay in the second phase (groups A and B, respectively, in Table 1). Thus, P11, P12, P9, P16, and P2 (group A) show a fast first phase (mean  $t_{1/2} = 23.6$  hours), followed by a slower second-phase decline (mean  $t_{1/2} = 7.2$  days); whereas P7, P18, P17, P15, P19, P14, and P10 (group B) show a fast first phase (mean  $t_{1/2} = 19.3$  hours), followed by a flat second phase. We note that there is no statistical difference between the first-phase half-lives of these

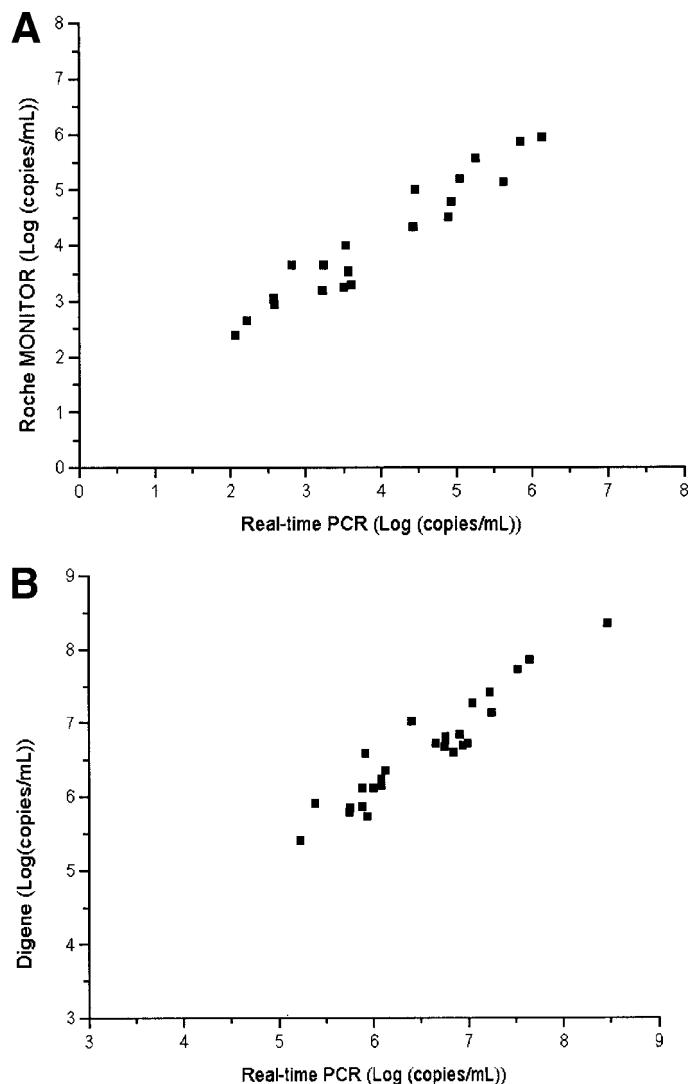


FIG. 3. Comparison of HBV viral load for HBV-infected serum samples by the molecular-beacon based real-time PCR assay and the Roche COBAS HBV AMPLICOR MONITOR assay (A,  $n = 20$ ,  $P < .001$ ) and the Digene Hybrid Capture II assay (B,  $n = 26$ ,  $P < .001$ ).

2 groups ( $P > .3$ ). In Table 1, we also show a third group of individuals (group C) for whom there are not enough data to accurately calculate the rate of decay of both the first and second phases. For instance, for P6 the first data point is at 15 days into treatment and a calculation of the first-phase decay is not possible. For P3 and P13, the follow-up period is too short for conclusions about the second phase. Also, even though we have classified patient P7 in group B based on the decay profile obtained by data fitting, it is possible that this case represents a nonresponder, with a viral load decrease of 1 log, followed by a very slow increase over the time of treatment (Fig. 4A). Note that this individual had the lowest baseline viral load and was in the LMV-alone arm of the study.

The slope of the first phase of HBV DNA decay is also variable—ranging, with one exception, between 17 hours and 92 hours—and is not associated with the type of treatment, pretreatment concentration of HBV DNA, or alanine transaminase (ALT) level. It can be shown from equation 2 that when  $\delta \ll c$ , the decay slope is given by the product of the virion clearance rate,  $c$ , and the drug efficacy,  $\epsilon$ . Because drug effi-

cacy is greater than 0.9 in all but 1 patient (Table 1), the major determinant of the variation in the first-phase slope is differences in virion clearance rate. In one individual, P11, an abrupt decrease in viral load can be observed. Between day 1 and day 3, the viral titer of this individual decreases 1.5 log, which corresponds to a viral half-life of about 1 hour. Thus, even though there is some uncertainty in this measure, because there are only 3 data points (days 1, 2, and 3), it seems that viral clearance can be much faster than previously thought<sup>31</sup> and comparable with that observed for HIV and HCV.<sup>10</sup> The second phase, which in our model is associated with the loss of infected cells, also shows heterogeneity with half-lives as short as 2.4 days (for P12), and in other individuals there is no decay. Previous studies have always suggested a second-phase decline; however, it is clear from these new data that, with more measurements in the second phase, many individuals do not show any decline over a period of 2 months after the first phase. Also, there is no association between the slope of the second phase and the type of treatment, pretreatment concentration of HBV DNA or ALT.

*Some Individuals Exhibit a Complex Multiphasic "Staircase" Pattern of Decay.* The HBV decay patterns may not always be biphasic. For example, several individuals seem to have a staircase pattern in the decay of viral load (Fig. 5). After the administration of antiviral therapy to patient P11, between day 1 and day 3 there is a very fast decay of about 1.5 log, which is followed by a long constant phase (within 0.5 log) until day 39. Then there is a further 3 log drop in the next 2 weeks, again followed by a plateau that lasts until the end of the study on day 81. It should be noted, that no changes in treatment protocol were implemented that might explain this pattern. Moreover, if this pattern were caused by noncompliance or treatment cessation, we would expect to see rapid viral rebound<sup>5</sup> (as seen in all individuals following cessation of therapy after 80 days, data not shown). However, partial drug compliance is a possibility that we are unable to exclude. We were also unable to show the development of a mutation at position 526 or 550 that is associated with antiviral resistance during this plateau phase (data not shown). Hence the observed staircase pattern appears intrinsic to the dynamics of viral titer decrease. This may also be the case in patients P9, P6, P3, and P18 (Fig. 5).

*A Subset of Individuals Shows a Long Delay Before the Initial Decay of Viral Load Under Treatment.* The fitting of the data to the model allowed for a delay between the start of treatment and the initial decay of viral load (see Model Description). The average delay was 1.6 days, but some individuals showed much longer delays (for example P9 had a delay of 5 days [Fig. 4A]). In contrast, in a few individuals (e.g., P15) no delay could be detected. It is likely that the delay is larger in the group treated with LMV alone (mean, 2.2 days) than in the combination therapy group (mean, 1.3 days); however, this difference was not significant ( $P > .1$ ).

In many individuals, the delay in decline in viral load is associated with a transient increase in viral load at the start of treatment (see patients P9, P14, or P16). This increase may be caused by random fluctuations. However, in P9 there is a sustained increase over a period of 5 days; in P14 there is a 1.5 log increase, which is larger than the usual random fluctuations in viral load; and in P16 there are 4 data points before the start of treatment indicating a very stable viral load of 3 to 4  $\times 10^8$ /mL for 80 days, before the

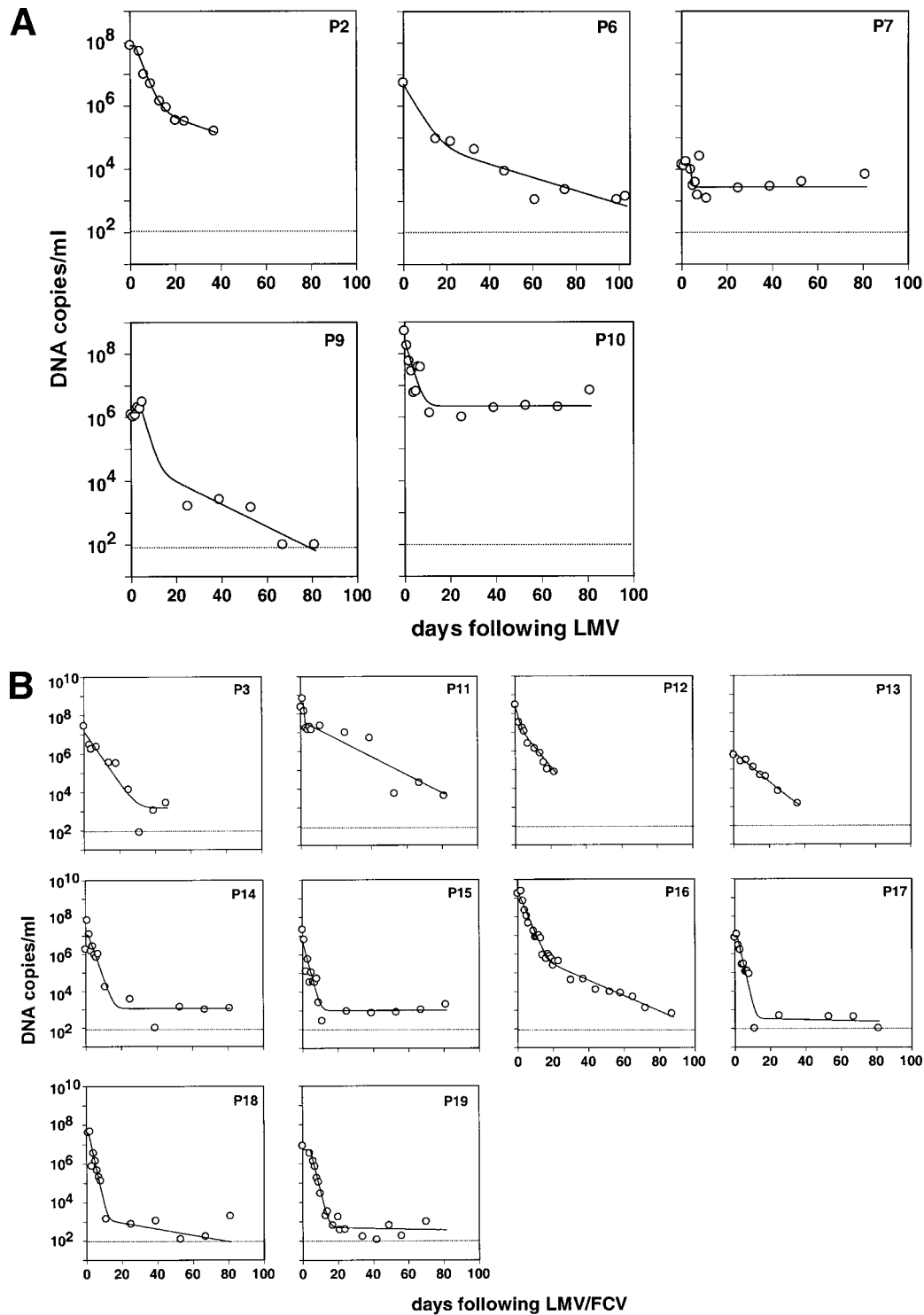


FIG. 4. Results of fitting the model to the data. The data points are represented by symbols, and the lines show the best fit of the data to the mathematical model. The best estimates for the fitted parameters are shown in Table 1. (A) Individuals treated with lamivudine. (B) Individuals treated with a combination of LMV and FCV. The horizontal line indicates the limit of detection (100 copies/mL).

increase at the start of therapy. These observations strongly indicate that this increase in viral load is not caused by random fluctuations and suggest that they may be due to some early effect of the drug treatment itself. Similar increases were observed when HIV-1-infected individuals started antiretroviral therapy.<sup>32</sup>

**LMV/FCV Combination Therapy Is Associated With Greater HBV Antiviral Efficacy.** The major difference between combination and monotherapy was a significantly greater drop in viral load with LMV/FCV combination compared with LMV alone

( $5.20 \pm 0.25$  vs.  $2.94 \pm 0.67$  log drop,  $P < .01$ ), which is reflected in a significantly greater antiviral efficacy associated with combination therapy ( $\epsilon = 0.985$  vs.  $0.951$ ,  $P = .042$ ). There was no evidence of resistance to LMV given that wild-type M550 was detected both before and after therapy in all individuals. Resistance to FCV, as shown by the L526M mutation, was more frequently detected, occurring in 4 of 5 individuals in the monotherapy arm and 1 of 10 individuals in the combination therapy arm. However, this mutation does not seem to have affected the dynamics of viral decay because

TABLE 1. Demographic and Viral Dynamic Data

	Gender/Age (yr)	Treatment Regimen	ALT <sub>0</sub> (IU/mL)	HBeAg (end 12W treatment)	Amino Acid at Position 526*	Log Drop Viral Load (log copies/mL)	V <sub>0</sub> (copies/mL)	Efficacy	t <sub>1/2</sub> First Phase (h)	t <sub>1/2</sub> Second Phase (d)	τ Delay (d)
Group A											
P11	M/25	LMV/FCV	48	Pos	L526	5.19	3.91E + 08	0.9102	1.0	5.7	1.9
P12	M/30	LMV/FCV	420	Neg	L526M	NA	2.53E + 08	0.9415	17.6	2.4	0.0
P9	F/30	LMV	84	Pos	L526	4.09	1.61E + 06	0.9822	29.3	8.5	5.0
P16	M/18	LMV/FCV	920	Neg	L526	6.44	1.74E + 09	0.9993	31.9	7.3	0.6
P2	M/27	LMV	308	Pos	L526M	NA	8.14E + 07	0.9890	38.3	12.0	2.2
Mean			356			5.24	4.93E + 08	0.9644	23.6	7.2	1.9
SE			157			0.68	3.19E + 08	0.0167	6.6	1.6	0.9
Group B											
P7†	F/30	LMV	251	Pos	L526M	1.07	1.47E + 04	0.8091	5.4	>120	3.8
P18	M/18	LMV/FCV	190	Pos	L526	5.59	4.19E + 07	0.9999	17.2	>120	1.3
P17	M/25	LMV/FCV	78	Pos	L526	4.42	8.99E + 06	0.9999	17.3	>120	1.3
P19	M/23	LMV/FCV	144	Pos	L526	5.00	1.15E + 07	0.9999	19.4	>120	4.3
P15	M/50	LMV/FCV	60	Pos	L526	4.89	5.17E + 06	0.9998	20.5	>120	0.0
P14	F/26	LMV/FCV	36	Pos	L526	4.85	1.14E + 07	0.9999	26.4	>120	1.4
P10	M/35	LMV	40	Pos	L526M	2.91	3.07E + 08	0.9917	29.0	>120	0.0
Mean			114			4.10	5.51E + 07	0.9715	19.3		1.7
SE			31			0.60	4.23E + 07	0.0271	2.9		0.6
Group C											
P6	M/32	LMV	180	Pos	L526M	3.69	5.47E + 06	0.9846	NA	14.3	0.0
P3	M/33	LMV/FCV	170	Pos‡	L526	NA	1.56E + 07	0.9999	53.7	NA	0.0
P13	F/49	LMV/FCV	90	Pos	L526	NA	5.70E + 05	0.9995	91.9	NA	1.9
Overall mean			201			4.38	1.92E + 08	0.9738	28.5		1.6
Overall SE			59			0.44	1.15E + 08	0.0135	6.0		0.4

NOTE. ALT<sub>0</sub> = ALT levels before the start of therapy; HBeAg is shown at the end of 12 weeks of treatment, we note that all patients were HBeAg-positive before the start of therapy; V<sub>0</sub> = HBV viral load at baseline. Log viral load drop was only calculated for individuals in whom viral load was known at 12 weeks and who were on treatment for 12 weeks. Group A, fast first-phase and second-phase responders; group B, fast first-phase and no second-phase decay; group C, patients for whom data is lacking for an accurate measurement of either first- or second-phase decay.

Abbreviations: Pos, positive; Neg, negative; NA, not available.

\*Determined by line probe assay. L526 (leucine) and L526M (methionine) at position 526. All individuals demonstrated M550, i.e., all were sensitive to LMV.

†Patient was fitted without data from day 8 by jackknife method. Also, although P7 is in group B, he or she may be a nonresponder.

‡Transient *e* seroconversion.

it was detected in the same proportion of individuals with a first-phase decline faster than 24 hours (2 of 7) and slower than 24 hours (3 of 8). An L526M mutation was detected before treatment in 2 of 9 individuals with a flat second phase, i.e., a long half-life of infected cells (>120 days).

DISCUSSION

We have introduced a new technique that uses molecular beacons and real-time PCR<sup>16,17</sup> to measure HBV viral titers.

This technique provides accurate results over a range of serum HBV DNA concentrations, varying between 10<sup>2</sup> and 10<sup>9</sup> copies/mL. We have shown considerable variation in the response to HBV treatment, both with LMV alone and combination therapy. This variation may have been present in previous studies. For example, in the work by Tsiang et al.<sup>7</sup> the data from patients C and F in their Fig. 2 show a fast first phase followed by what could be a flat second phase, similar to our patients in group B (Table 1). Although in Tsiang et al.,<sup>7</sup>

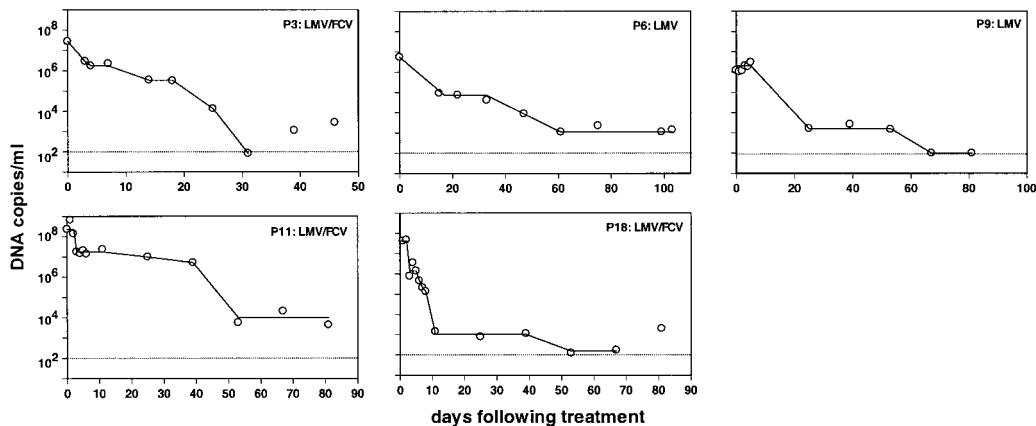


FIG. 5. A “staircase pattern” of HBV DNA decay is seen in 5 individuals. The lines correspond to the “steps” of the “staircase.”

patients C and F were estimated to have a second-phase decay half-life of 30 and 20 days, respectively, and thus are not strictly representative of our group B, they both show 3 flat measurements between about 55 and 90 days post-therapy. In addition, the data for patients A, B, and J in Tsiang et al.<sup>7</sup> show systematic deviations from the biphasic model, and by simply connecting points the data could be viewed as being consistent with a staircase pattern of viral load decline, similar to patient P11 in this report. It is possible that the detection of diverse declines in HBV viral load in our study reflects differences in the patient inclusion criteria, namely, individuals with both high and low viral loads and individuals with varying abnormality in liver function, as reflected by a wide range in ALT levels (range, 36-920). Alternatively, the observed heterogeneity in this study may be related to the dynamic range of the real-time PCR-based assay, whereby more accurate quantification can be performed at high viral loads (when compared with the HBV MONITOR assay used in Nowak et al.<sup>5</sup> and Zeuzem et al.<sup>6</sup>) or low viral loads (when compared with the Digene assay in Tsiang et al.<sup>7</sup>). The ability to quantify HBV DNA over a wide dynamic range allows a more accurate description of both the first- and second-phase viral load declines within the same patient.

At a deeper level, the reason for this variation among individuals may lie in the important immunologic component of HBV infection. HBV is thought to be primarily a noncytotoxic virus, and infected cells are lost either through death, mainly immune-mediated killing, or via "cure," *i.e.*, loss of cccDNA.<sup>25</sup> The second-phase decay has been associated with the rate of loss of productively infected cells.<sup>7</sup> Thus, the plateau we observe in the second phase may be explained by a delayed or weak immune response, which slows the loss of infected cells. Initially, antiviral therapy partially blocks the production of new virions and there is a rapid decline of plasma HBV DNA, but a vigorous immune response may be needed to drive the second-phase decline, which involves the loss of cells still producing virus. In those individuals who have difficulty mounting this response, a very slow decline or even no decline at all may be observed. The same reasoning may explain the pattern we called "staircase." One hypothesis is that initially these individuals have a poor immune response, so that therapy simply reduces viral production per cell, but not the number of infected cells. This leads to the decay in virus and then a leveling off as a new equilibrium is reached. If the new equilibrium were 2 logs below the baseline viral load, then the drug efficacy in blocking production,  $\epsilon$ , would be 99%. This indicates that on average infected cells still produce 1% as much virus as before therapy.

If an immune response is initiated or intensified, in the presence of reduced viral load, then the number of infected cells would decrease leading to a further decrease in viral load. In this context, reductions in viral load to less than  $10^4$  DNA copies/mL have been shown to correlate with HBeAg seroconversion, but it remains unclear if this is indeed associated with enhanced clearance of infected cells or long-term suppression of viral disease.<sup>33</sup> This hypothesis is also consistent with the recent report that LMV therapy can result in improved T-cell function, by as yet unknown mechanisms.<sup>34</sup> Unfortunately this is difficult to test, because in this and another study<sup>34</sup> the putative increase in the immune response does not correlate with HBeAg seroconversion. In addition, in our patients the

staircase pattern for viral decay does not correlate with the levels of ALT before therapy or during therapy (data not shown). For the individuals with this staircase pattern (Figure 5), P9 and P11 had low levels of ALT before therapy, whereas P3, P6, and P18 had high levels. Thus, to explain the "third phase" in these individuals, one may need to invoke regulatory interactions that can lead not only to enhanced cytolytic, but also to noncytolytic mechanisms of loss of HBV-infected cells or further cytokine-mediated reductions in viral production. Alternatively, as has been proposed for HIV, 2 or more populations of infected cells may exist with differing lifespans.<sup>3</sup> Populations of infected cells may also be heterogeneous with respect to their expression of drug efflux pumps such as P-glycoprotein and the newly discovered family of multidrug resistance-associated proteins (MRPs). Interestingly, overexpression of MRP-4 in a human T-cell line has been shown to impair the anti-HIV activity of the nucleoside reverse transcriptase inhibitors adefovir, zivovudine, and LMV.<sup>35,36</sup> If similar effects occur in hepatocytes, then multiple steady states could arise leading to a step-wise decline. For example, cells with low or normal expression levels of MRP-4 might be inhibited from producing HBV early in therapy, and then either with increased drug levels as dosing continued or the death of high-expressing MRP-4 cells, further inhibition of HBV production could be observed leading to a new lower steady state. Also, if HBV can reversibly bind to follicular dendritic cells in secondary lymphoid organs (*i.e.*, spleen and lymph nodes) as HIV does, then additional complexities arise in interpreting viral decay curves.<sup>37</sup> If any of these effects were significant, then HBV viral decay after therapy may not be adequately described by biphasic curves.

The heterogeneities observed also have implications for the way HBV dynamics should be modeled. In the analyses by Nowak et al.<sup>5</sup> and Tsiang et al.,<sup>7</sup> the investigators assumed that treatment stops all new infections, that is  $\eta = 1$ . LMV and FCV act primarily by reducing new virion production and they may have little effect in blocking infection. Thus,  $\eta$  should be small compared with 1. The assumption  $\eta = 1$  has been made before, because it simplifies the theory, and analysis of the model shows that  $\eta$  has little effect on the quality of the fits to the data and the resulting parameter estimates. For example, we found that fitting the data assuming  $\eta = 0$  or  $\eta = 1$  yields similar estimates for  $c$ ,  $\delta$ , and  $\epsilon$ , with differences of less than 5% between the 2 scenarios. The case  $\eta = 1$  results in a slight overestimate of  $c$  and underestimate of  $\delta$  and  $\epsilon$ , compared with assuming  $\eta$  is less than 1. Nevertheless, it is biologically more realistic to use the assumption that  $\eta$  is less than 1. In addition to biochemical data pointing to  $\eta$  being less than 1,<sup>26-28</sup> in this study 7 of 15 patients under therapy, both with LMV alone and in combination with FCV, did not show a second-phase decline. It is clear from the analysis of model 1 that if  $\eta = 1$ , then theoretically this flat phase cannot be reached, and during therapy the viral decay continues until  $V = 0$ . On the other hand, if  $\eta$  is less than 1, theoretically a new steady state may be reached when the rate of creation of new infected cells balances their rate of loss, *i.e.*,  $(1 - \eta)BVT = \delta I$ . Such a steady state exists only for the full 3-equation model (equation 1), but not for the model with constant target cells, with equation 2 as a solution. For example, numerically solving the system of equations 1 with parameters  $V(0) = 1.5 \times 10^7$  copies/mL,  $I(0) = 9 \times 10^{10}$  cells,  $T(0) = 10^{10}$  cells,

$c = 0.7 \text{ day}^{-1}$ ,  $\delta' = 0.1 \text{ day}^{-1}$ ,  $\rho = 0 \text{ day}^{-1}$ ,  $\eta = 0.5$ , and  $\epsilon = 0.7$  leads to this new infected steady state. A more detailed mathematical analysis of model 1 will be published elsewhere.

In analyzing the complete model, we introduced parameters characterizing target cell kinetics and could no longer lump the death rate,  $\delta'$ , and the rate of reversion to the uninfected state,  $\rho$ , in one parameter,  $\delta$ , because reversion now plays an important role. This increased the number of parameters and made simultaneous estimation of all the parameters impossible. Nevertheless, with the full model we could show that with  $\eta$  less than 1, a flat second phase could occur even when the death rate of infected cells was non-zero.

The free virion clearance rate,  $c$ , was found to be more variable in the individuals studied than previously reported. In addition, for one individual, clearance was very rapid corresponding to a virion half-life of 1 hour, similar to the fast clearance seen in HIV<sup>10</sup> and HCV<sup>4,10</sup> infections. One potential difference between the clearance of HIV and HCV and that of HBV is the higher viral loads characteristic of HBV infection and the presence of huge quantities (e.g.,  $10^{13}/\text{mL}$ ) of noninfectious 22-nm spherical and filamentous particles, which lack HBV DNA.<sup>27</sup> If the liver is indeed a major site of virion clearance,<sup>20</sup> reduced HBV clearance may be due to defects in reticuloendothelial function, possibly related to the degree of liver inflammation, portal hypertension, or the high particle concentrations, which may overburden and slow the clearance mechanisms. Detailed measurements of the concentration of the 22-nm noninfectious particles in the sera of infected individuals could shed light on this issue.

An important difference between our model and those proposed in previous studies is the inclusion of an initial delay before drug therapy has an effect. This delay is clearly seen in many individuals in this study, and there is a trend toward more prolonged delays in individuals taking monotherapy. Similar delays have been observed in studies of HIV and HCV drug treatment. Biologically they may correspond to the period required for drug uptake and activation by phosphorylation. However, the delays measured here are frequently too long to be explained by simple pharmacokinetics. Whatever the explanation, these delays have an important role in the fitting of the data. In fact, not taking them into account results in an underestimate of the rate of virion clearance. In future studies, more frequent sampling at the early stages of treatment would help refine estimates of the delay and the virion clearance rate.

Finally, this study has confirmed the potency of LMV in blocking new virus production with efficacy of the order of 95%, and that this can be increased by the use of combination therapy with LMV and FCV with efficacy increasing to values close to 99%.<sup>15</sup> Clinical trials are needed to assess the long-term benefits of combination therapy for the treatment of HBV-infected individuals, possibly also including an immune modulating cytokine such as interferon alfa in the regimen.

#### REFERENCES

- Wei X, Ghosh SK, Taylor ME, Johnson VA, Emini EA, Deutsch P, Lifson JD, et al. Viral dynamics in human immunodeficiency virus type 1 infection. *Nature* 1995;373:117-122.
- Ho D, Neumann A, Perelson A, Chen W, Leonard J, Markowitz M. Rapid turnover of plasma virions and CD4 lymphocytes in HIV-1 infection. *Nature* 1995;373:123-126.
- Perelson A, Essunger P, Cao Y, Vesanan M, Hurlley A, Saksela K, Markowitz M, et al. Decay characteristics of HIV-1-infected compartments during combination therapy. *Nature* 1997;387:188-191.
- Neumann AU, Lam NP, Dahari H, Gretch DR, Wiley TE, Layden TJ, Perelson AS. Hepatitis C viral dynamics in vivo and the antiviral efficacy of interferon-alpha therapy. *Science* 1998;282:103-107.
- Nowak MA, Bonhoeffer S, Hill AM, Boehme R, Thomas HC, McDade H. Viral dynamics in hepatitis B virus infection. *Proc Natl Acad Sci U S A* 1996;93:4398-4402.
- Zeuzem S, de Man RA, Honkoop P, Roth WK, Schalm SW, Schmidt JM. Dynamics of hepatitis B virus infection in vivo. *J Hepatol* 1997;27:431-436.
- Tsiang M, Rooney JF, Toole JJ, Gibbs CS. Biphasic clearance kinetics of hepatitis B virus from patients during adefovir dipivoxil therapy. *HEPATOLOGY* 1999;29:1863-1869.
- Haase A, Henry K, Zupancic M, Sedgewick G, Faust R, Melroe H, Cavert W, et al. Quantitative image analysis of HIV-1 infection in lymphoid tissue. *Science* 1996;274:985-989.
- Cavert W, Notermans D, Staskus K, Wietgreffe S, Zupancic M, Gedhard K, Henry K, et al. Kinetics of response in lymphoid tissues to antiretroviral therapy of HIV-1 infection. *Science* 1997;276:960-964.
- Ramratnam B, Bonhoeffer S, Binley J, Hurlley A, Zhang L, Mittler JE, Markowitz M, et al. Rapid production and clearance of HIV-1 and hepatitis C virus assessed by large volume plasma apheresis. *Lancet* 1999;354:1782-1785.
- Dienstag JL, Schiff ER, Wright TL, Perrillo RP, Hann HW, Goodman Z, Crowther L, et al. Lamivudine as initial treatment for chronic hepatitis B in the United States. *N Engl J Med* 1999;341:1256-1263.
- de Man RA, Marcellin P, Habal F, Desmond P, Wright T, Rose T, Jurewicz R, et al. A randomized, placebo-controlled study to evaluate the efficacy of 12-month famciclovir treatment in patients with chronic hepatitis B e antigen-positive hepatitis B. *HEPATOLOGY* 2000;32:413-417.
- Trepo C, Jezek P, Atkinson G, Boon R, Young C. Famciclovir in chronic hepatitis B: results of a dose-finding study. *J Hepatol* 2000;32:1011-1018.
- Gilson RJ, Chopra KB, Newell AM, Murray-Lyon IM, Nelson MR, Rice SJ, Tedder RS, et al. A placebo-controlled phase I/II study of adefovir dipivoxil in patients with chronic hepatitis B virus infection. *J Viral Hepat* 1999;6:387-395.
- Lau GK, Tsiang M, Hou J, Yuen S, Carman WF, Zhang L, Gibbs CS, et al. Combination therapy with lamivudine and famciclovir for chronic hepatitis B-infected Chinese patients: a viral dynamics study. *HEPATOLOGY* 2000;32:394-399.
- Tyagi S, Kramer FR. Molecular beacons: probes that fluoresce upon hybridization. *Nat Biotechnol* 1996;14:303-308.
- Lewin S, Vesanan M, Kostrikis L, Hurlley A, Duran M, Zhang L, Ho D, et al. The use of real-time PCR and molecular beacons to detect virus-replication in HIV-1-infected individuals on prolonged effective antiretroviral therapy. *J Virol* 1999;73:6099-6103.
- Shimizu Y, Feinstone S, Kohara M, Purcell R, Yoshikura H. Hepatitis C virus: detection of intracellular virus particles by electron microscopy. *HEPATOLOGY* 1996;23:205-209.
- Kaito M, Watanabe S, Tsukiyama-Kohara K, Yamaguchi K, Kobayashi Y, Konishi M, Yokoi M, et al. Hepatitis C virus particle detected by immunoelectron microscopic study. *J Gen Virol* 1994;75:1755-1760.
- Nathanson N, Tyler KL. Entry, dissemination, shedding, and transmission of viruses. In: Nathanson N, ed. *Viral Pathogenesis*. Philadelphia: Lippincott-Raven, 1997;13-33.
- Fink L, Seeger W, Ermert L, Hanze J, Stahl U, Grimminger F, Kummer W, et al. Real-time quantitative RT-PCR after laser-assisted cell picking. *Nat Med* 1998;4:1329-1333.
- Gibson UE, Heid CA, Williams PM. A novel method for real time quantitative RT-PCR. *Genome Res* 1996;6:995-1001.
- Heid CA, Stevens J, Livak KJ, Williams PM. Real time quantitative PCR. *Genome Res* 1996;6:986-994.
- Stuyver L, Van Geyt C, De Gendt S, Van Reybroeck G, Zoulim F, Leroux-Roels G, Rossau R. Line probe assay for monitoring drug resistance in hepatitis B virus infected patients during antiviral therapy. *J Clin Microbiol* 2000;38:702-707.
- Guidotti LG, Rochford R, Chung J, Shapiro M, Purcell R, Chisari FV. Viral clearance without destruction of infected cells during acute HBV infection. *Science* 1999;284:825-829.
- Kock J, Schlicht HJ. Analysis of the earliest steps of hepadnavirus replication: genome repair after infectious entry into hepatocytes does not depend on viral polymerase activity. *J Virol* 1997;67:4867-4874.
- Kann M, Gerlich W. Structure and molecular virology. In: Zuckerman AJ, Thomas HC, eds. *Viral Hepatitis*. London: Churchill Livingstone, 1998; 77-105.

28. Delaney WE, Miller TG, Isom HC. Use of hepatitis B virus recombinant baculovirus-HepG2 system to study the effects of (-)- $\beta$ -2',3'-dideoxy-3'-thiacytidine on replication of hepatitis B virus and accumulation of covalently closed circular DNA. *Antimicrobial agents and chemotherapy* 1999;43:2017-2026.
29. Loeb K, Jerome K, Goddard J, Huang M, Cent A, Corey L. High-throughput quantitative analysis of hepatitis B virus DNA in serum using the TaqMan fluorogenic detection system. *HEPATOLOGY* 2000;32:626-629.
30. Pas SD, Fries E, De Man RA, Osterhaus AD, Niesters HG. Development of a quantitative real-time detection assay for hepatitis B virus DNA and comparison with two commercial assays. *J Clin Microbiol* 2000;38:2897-2901.
31. Peek S, Cote P, Jacob J, Toshkov I, Hornbuckle W, Baldwin B, Wells F, et al. Antiviral activity of clevudine [L-FMAU, (1-(2-fluoro-5-methyl- $\beta$ -L-arabinofuranosyl) uracil)] against woodchuck hepatitis virus replication and gene expression in chronically infected woodchucks (*Marmota monax*). *HEPATOLOGY* 2001;33:254-266.
32. Perelson AS, Neumann AU, Markowitz M, Leonard JM, Ho DD. HIV-1 dynamics in vivo: virion clearance rate, infected cell life-span, and viral generation time. *Science* 1996;271:1582-1586.
33. Gauthier J, Bourne E, Lutz M, Crowther L, Dienstag J, Brown N, Condeelis LD. Quantitation of hepatitis B viremia and emergence of YMDD variants in patients with chronic hepatitis B treated with lamivudine. *J Infect Dis* 1999;180:1757-1762.
34. Boni C, Bertoletti A, Penna A, Cavalli A, Pilli M, Urbani P, Scognamiglio P, et al. Lamivudine treatment can restore T-cell responsiveness in chronic hepatitis B. *Journal of Clinical Investigation* 1998;102:968-975.
35. Schuetz JD, Connelly MC, Sun D, Paibir SG, Flynn PM, Srinivas RV, Kumar A, et al. MRP4: A previously unidentified factor in resistance to nucleoside-based antiviral drugs. *Nat Med* 1999;5:1048-1051.
36. Fridland A, Connelly MC, Robbins BL. Cellular factors for resistance against antiretroviral agents. *Antivir Ther* 2000;5:181-185.
37. Hlavacek W, Stilianakis N, Notermans D, Danner S, Perelson A. Influence of follicular dendritic cells on decay of HIV during antiretroviral therapy. *Proc Natl Acad Sci U S A* 2000;97:10966-10971.